

- cyanate), Leu-3a-PE (phycoerythrin), and Leu-2a-PerCP (peridinin chlorophyll protein), which recognize the CD2, CD4, and CD8 molecules, respectively (Becton Dickinson, San Jose, CA); 7E14-APC (allophycocyanin), which recognizes the CD4 protein (Exalpha, Boston, MA); and 12G5-PE, which recognizes the CXCR4 protein (Pharmingen, San Diego, CA). The mAb FN-18-FITC, which recognizes the monkey CD3 molecule, was also used (Biosource International, Camarillo, CA). Absolute CD4 and CD8 cell counts were measured with TruCount absolute count tubes (Becton Dickinson, Mountainview, CA) according to the manufacturer's instructions. Flow cytometry analysis was performed with the FACS Calibur.
13. J. M. Harouse and C. Cheng-Mayer, unpublished data.
 14. H. Deng, D. Unutmaz, V. N. Kewal-Ramani, D. R. Littman, *Nature* **388**, 296 (1997); M. Farzan *et al.*, *J. Exp. Med.* **186**, 405 (1997); G. Alkhatib *et al.*, *Nature* **388**, 238 (1997).
 15. J. M. Harouse *et al.*, *Virology* **248**, 95 (1998).
 16. R. S. Veazey *et al.*, *Science* **280**, 427 (1998); J. J. Mattapallil *et al.*, *J. Virol.* **72**, 6421 (1998); Z. Smit-McBride *et al.*, *J. Virol.* **72**, 6646 (1998).
 17. Jejunal resectioning and anastomosis were performed by excising about 20 cm of intestinal tissue [D. Slatter, *Textbook of Small Animal Surgery* (Saunders, Philadelphia, ed. 2, 1993), vol. 1]. We dissected Colonic nodes from colonic mesentery and took ileal wedge biopsies from the antimesenteric side of the intestine followed by closure with a nylon suture. Surgical samples were processed within 30 min of the procedure. All surgical procedures were performed on anesthetized animals and were approved by IACUC.
 18. R. S. Veazey *et al.*, *Clin. Immunol. Immunopathol.* **82**, 230 (1997). In this study, the range of CD4⁺ jejunal LPLs in normal adult rhesus macaques was 34.3% to 56.9%, with a corresponding CD4-CD8 ratio of 0.88 ± 0.22 ($n = 4$).
 19. T. Schneider *et al.*, *Gut* **37**, 524 (1995).
 20. C. Bleul, L. Wu, J. A. Hoxie, T. A. Springer, C. R. Mackay, *Proc. Natl. Acad. Sci. U.S.A.* **94**, 1925 (1997); R. D. Berkowitz, K. P. Beckerman, T. J. Schall, J. M. McCune, *J. Immunol.* **161**, 3702 (1998).
 21. J. A. Zack *et al.*, *Cell* **61**, 213 (1990).
 22. P. Trivedi *et al.*, *J. Virol.* **70**, 6876 (1996); T. Zhu *et al.*, *ibid.*, p. 3098.
 23. Supported in part by National Institutes of Health grants AI41945 and CA72822. We thank D. D. Ho, R. Connor, R. Liu, S. Monard, and J. Segal (Aaron Diamond AIDS Research Center); R. Bohm, L. Martin, M. Ratterree, and the animal care staff at Tulane Regional Primate Research Center; R. Koup (University of Texas, Southwestern); P. J. Dailey, L. Sawyer, and J. Booth (Chiron Diagnostics); and R. Veazey (New England Regional Primate Research Center).

12 February 1999; accepted 26 March 1999

Chemokine Up-Regulation and Activated T Cell Attraction by Maturing Dendritic Cells

H. Lucy Tang and Jason G. Cyster*

Langerhans' cells migrating from contact-sensitized skin were found to up-regulate expression of macrophage-derived chemokine (MDC) during maturation into lymph node dendritic cells (DCs). Naïve T cells did not migrate toward MDC, but antigen-specific T cells rapidly acquired MDC responsiveness *in vivo* after a subcutaneous injection of antigen. In chemotaxis assays, maturing DCs attracted activated T cells more strongly than naïve T cells. These studies identified chemokine up-regulation as part of the Langerhans' cell maturation program to immunogenic T cell-zone DC. Preferential recruitment of activated T cells may be a mechanism used by maturing DCs to promote encounters with antigen-specific T cells.

Skin DCs, or Langerhans' cells (LCs), form an extensive network in the epidermis, and upon exposure to noxious stimuli such as lipopolysaccharide (LPS) or to contact sensitizers such as fluorescein isothiocyanate (FITC), they enter lymphatics and migrate into T cell zones of lymph nodes to become interdigitating DCs (1). For mature DCs to function in an immunogenic manner, it is important that they rapidly interact with antigen-specific T cells. One mechanism that may enhance encounters between DCs and T cells is for DCs to produce T cell-attracting chemokines. Although DCs express several chemokines (2–5), it has not been established whether immature DCs such as LCs up-regulate chemokine expression during *in vivo* maturation to immunogenic DCs.

Macrophage-derived chemokine (MDC) is highly expressed in lymphoid tissues (5–8). To characterize its expression in more detail, we isolated the mouse MDC homolog

and used it to probe lymphoid tissues by *in situ* hybridization (9). Multiple strongly hybridizing cells were identified in T cell zones of lymph nodes (Fig. 1B), whereas only occasional cells hybridized in the spleen (Fig. 1A). Frequently, the MDC-expressing cells were concentrated in regions of the T cell zone proximal to follicles (Fig. 1B), which are areas rich in DCs (1), and under higher magnification, they demonstrated a dendritic morphology (Fig. 1C). Consistent with the *in situ* data and with findings by others (5–8), Northern (RNA) blot analysis showed that MDC was highly expressed in lymph node DCs (Fig. 1D) and was undetectable in DC-depleted lymph nodes or in peritoneal macrophages (Fig. 1D). To test for the production of MDC protein, we incubated purified lymph node DCs *in vitro* to allow chemokine secretion, and we tested the culture supernatant for the attraction of mouse CC-chemokine receptor 4 (CCR4)-transfected cells (10–13). A chemotactic response was observed with transfected but not with control cells (Fig. 1E). In addition to making MDC, we found, in preliminary studies (14), that lymph node DCs express thymus- and activation-regulated chemokine

(TARC), which is a second CCR4 ligand (15), and it is possible that TARC contributes to the CCR4 cell attractant activity made by DCs.

After the exposure of skin to contact sensitizers, LCs migrate to lymph nodes but do not enter circulation or migrate to the spleen (1, 16, 17), raising the possibility that the MDC-expressing DCs in lymph nodes might be LC derived. We therefore tested whether exposure to the contact sensitizer FITC resulted in changes in lymph node MDC expression. One day after skin was painted with FITC (18), MDC expression in draining lymph nodes was increased threefold (Fig. 2A), and it remained elevated over the next 2 days (Fig. 2A). In contrast, no increase in MDC occurred in the spleen after an intravenous injection of LPS (Fig. 2A), a treatment that promotes the migration of DCs from the splenic marginal zone to the T cell zone (19). In agreement with previous studies (20), FITC⁺ major histocompatibility complex (MHC) class II⁺ DCs could be detected among cells from lymph nodes draining a site of skin painted with FITC, and these DCs were absent from nondraining nodes (Fig. 2B). A microscopic analysis of isolated DCs showed that the FITC was concentrated within intracellular compartments (Fig. 2C). When day one draining lymph nodes were sectioned and stained to identify B and T cell zones, small numbers of brightly fluorescent FITC⁺ cells could be identified within the T cell zone but not in follicles (Fig. 2D). Combining this technique of tracking migrating DCs with *in situ* hybridization for MDC (9), we found that it was possible to establish that many of the FITC-bearing cells in the T cell zone were strongly positive for MDC expression (Fig. 2E). Reverse transcriptase-polymerase chain reaction (RT-PCR) analysis of sorted FITC⁺ lymph node DCs (21) confirmed that MDC was expressed in these cells (Fig. 3A). In contrast, EBI-1 ligand chemokine (ELC), a chemokine expressed constitutively by a subset of T cell zone DCs (4), was not detectable among FITC⁺ DCs (Fig. 3A).

Department of Microbiology and Immunology, University of California at San Francisco, San Francisco, CA 94143, USA.

*To whom correspondence should be addressed. E-mail: cyster@itsa.ucsf.edu

REPORTS

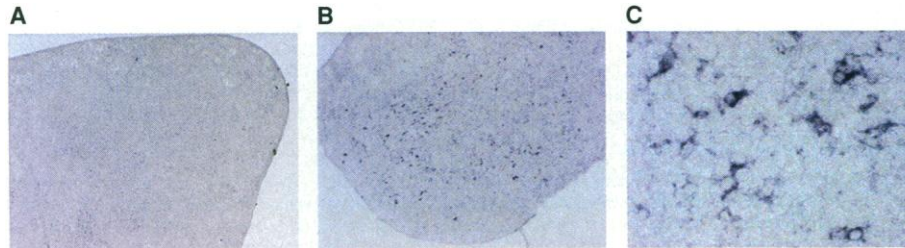


Fig. 1. MDC expression by DCs in lymph nodes. (A through C) Bright-field micrographs showing hybridization of the mouse spleen (A) and lymph node (B and C) with an antisense RNA MDC probe. Objective magnifications are $\times 5$ (A and B) and $\times 40$ (C). (D) Northern blot analysis of MDC mRNA in total lymph node (LN), lymph node cell suspension depleted of CD11c⁺ DCs (LN - DC), metrizamide-enriched lymph node DCs (DC), purified B and T cells, and day 7 thioglycollate-elicited peritoneal macrophages (Mac). Elongation factor-1 (EF-1) hybridization indicates relative amounts of RNA in each lane. (E) Chemotactic response of CCR4-transfected cells but not vector control cells to MDC or lymph node DC culture supernatant (DC s/n) that was prepared as described (27).

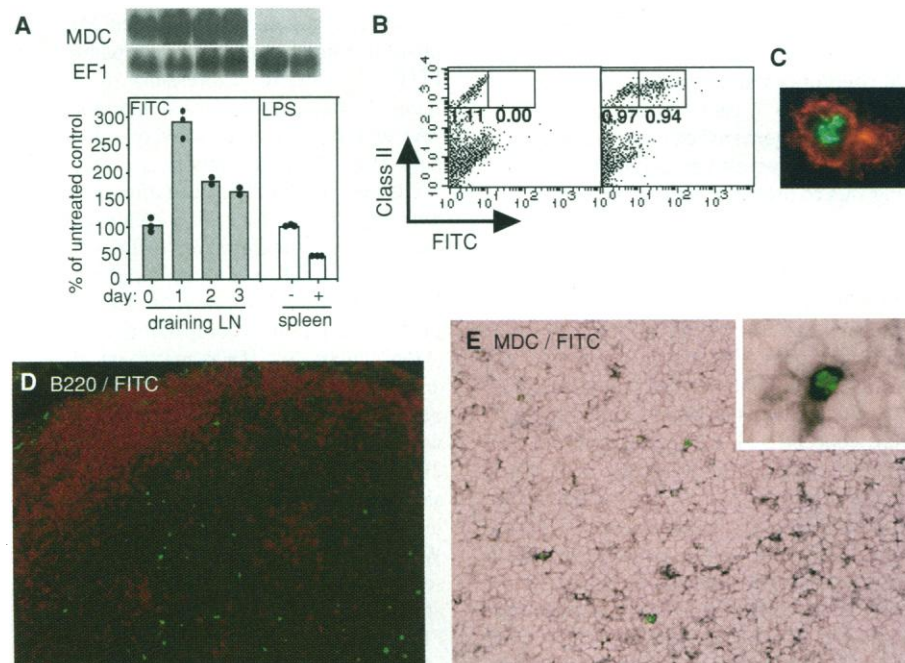


Fig. 2. Up-regulation of MDC by DCs migrating from FITC-sensitized skin to the T cell zone of lymph nodes. (A) Northern blot analysis of MDC in draining lymph nodes at days 0, 1, 2, and 3 after FITC skin painting (18) and in the spleen 1 day after intravenous injection of phosphate-buffered saline (-) or 35 μ g of LPS (+). Top panels show Northern blot analysis probed with MDC and EF-1, and the bottom panel displays the relative change in MDC expression in comparison to untreated mice. (B) Flow cytometric analysis of draining lymph node cells 1 day after FITC skin painting (right) and from the contralateral node (left) showing FITC fluorescence and MHC class II expression. Profiles shown are gated for B220⁺ cells. Numbers indicate the percentage of total cells within the overlying gate. (C) Dual-color fluorescence microscopy of isolated FITC⁺ lymph node DCs stained in red with anti-MHC class II biotin and streptavidin-Cy3. (D) Fluorescence microscopy of a day 1 draining lymph node section showing B220-stained B cell areas (red) and FITC fluorescence by DCs within the T cell zone. Objective magnification is $\times 10$. (E) Combined bright-field and fluorescence microscopy of a day 1 draining lymph node section after MDC in situ hybridization showing MDC expression (black) and FITC fluorescence. Objective magnification is $\times 10$ in the main panel and $\times 40$ in the inset.

Thus, many LCs express MDC but not ELC as they migrate into lymph node T cell zones to become mature DCs.

To determine whether MDC was already expressed by LCs in the skin or whether expression was up-regulated upon maturation, we prepared cell suspensions from epidermal sheets and cultured them to allow LC maturation (21, 22). About 3% of epidermal cells are MHC class II⁺ DCs (22), a frequency similar to the DC frequency in lymph nodes (1). Northern blot analysis detected an MDC signal in lymph node RNA, but it only detected a weak signal in RNA from freshly isolated epidermal cells (Fig. 3B), establishing that LCs do not constitutively express substantial amounts of MDC. However, after 4 hours of in vitro maturation, MDC expression began to increase (Fig. 3B), and by 2 days, a 150-fold up-regulation had occurred (Fig. 3B). High MDC expression was also detected by RT-PCR in LCs sorted from day 2 epidermal cell cultures (Fig. 3A). In contrast, ELC was not up-regulated in either the epidermal cell suspension or the sorted LCs (Fig. 3, A and B). The kinetics of MDC up-regulation were similar to the time required in vivo for maturing LCs to reach the T cell zone of draining lymph nodes (20), supporting the notion that MDC contributes to the function of LCs that have matured to T cell-zone DCs.

The expression of MDC by DCs draining into lymph nodes suggested a role in attracting T cells into contact with antigen-bearing DCs. Chemotaxis studies have demonstrated that MDC is not chemotactic for naïve or memory T cells but that MDC can attract T cells that have been activated in vitro and allowed to rest for several days, with repeated rounds of activation and rest improving the response (6-8, 23). To better define if T cells may be able to respond to MDC during the early phase of an immune response, we tested MDC responsiveness of in vivo activated

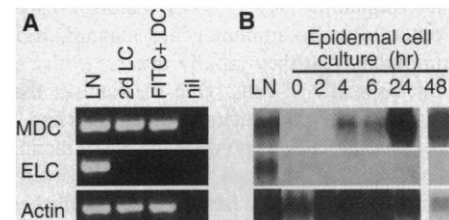


Fig. 3. Presence of MDC but not ELC expression by FITC⁺ lymph node DCs and cultured LCs. (A) RT-PCR analysis for MDC and ELC in total lymph node cells (LN), sorted MHC class II⁺ LCs that had been cultured for 2 days (2d LC), and sorted FITC⁺ MHC class II⁺ B220⁻ DCs from draining lymph nodes 1 day after skin painting (FITC⁺ DC). Actin RT-PCR is shown as a loading control. (B) Northern blot analysis of MDC and ELC expression in RNA from freshly prepared epidermal cells (0 hours) and from epidermal cells that were cultured for 2, 4, 6, 24, and 48 hours. RNA from the lymph node is included for comparison.

ovalbumin (OVA)-specific T cells (24, 25). A striking up-regulation in chemotaxis among OVA-specific T cells in draining lymph nodes was observed 2 days after immunization (Fig. 4A), which is a time when many of the cells have been activated (25), whereas OVA-specific T cells in nondraining nodes did not respond (Fig. 4A). Although the activated T cells remained responsive for 5 days after immunization (Fig. 4B), the response was not increased in comparison to that at day 2, indicating that the acquisition of MDC responsiveness is an early event in vivo T cell activation.

To determine whether MDC was representative of the overall chemoattractant profile of LC-derived DCs, we tested the ability of these cells to attract naïve and activated T cells. FITC⁺ DCs from lymph nodes draining

FITC-painted skin were cultured in vitro for 1 day to allow chemokine secretion (21), and the culture supernatant was used in chemotaxis assays. A chemotactic response was observed among activated T cells (Fig. 4C), whereas naïve T cells responded weakly or not at all (Fig. 4D). The addition of MDC to the activated T cells to desensitize CCR4 caused a partial reduction in their chemotactic response, indicating that MDC (and possibly TARC) makes a contribution to the chemokine activity but also that the DCs make other chemokines that attract activated T cells (Fig. 4C). To establish whether our assay system was able to detect the production of naïve cell attractants, we tested supernatants from cultures of lymph node stromal cell preparations (21) that contained cell types constitutively expressing known attractants of naïve cells, including secondary lymphoid-tissue chemokine (SLC) and ELC (26). These supernatants were active in attracting naïve CD4 T cells (Fig. 4D), whereas they had little activity for activated cells (Fig. 4C).

Our findings add up-regulation of T cell-attracting chemokine expression to the program of events that accompany LC maturation to immunogenic T cell-zone DCs. It is likely that other types of immature DCs up-regulate MDC during maturation as MDC is detected within mesenteric lymph nodes (14) that do not receive LCs from skin but that do contain DCs from intestinal epithelium (27). We propose that there are two phases of chemokine involvement in the early part of the T cell response in lymphoid tissues. In the first phase, maturing DCs and naïve T cells are attracted into the T cell zone by constitutively expressed chemokines such as SLC and ELC (26). Brought together in this way, antigen-loaded DC can prime rare antigen-specific T cells. In the second phase, activated and dividing T cells migrate more efficiently than the surrounding naïve T cells toward other newly arriving antigen-bearing DCs that produce chemokines such as MDC. This second phase should enhance the chance of encounter between antigen-specific T cells and antigen-bearing DCs. A similar mechanism of activated T cell attraction is likely to be used by antigen-bearing B cells (8). Expression of chemokines that differentially attract subsets of activated CD4 T cells (3, 7, 23) may also help different DC types to amplify polarized T cell responses.

References and Notes

1. J. Banachereau and R. M. Steinman, *Nature* **392**, 245 (1998); R. M. Steinman, M. Pack, K. Inaba, *Immunol. Rev.* **156**, 25 (1997); K. Shortman and C. J. Caux, *Stem Cells* **15**, 409 (1997).
2. G. J. Adema et al., *Nature* **387**, 713 (1997).
3. F. Sallusto, D. Lenig, C. R. Mackay, A. Lanzavecchia, *J. Exp. Med.* **187**, 875 (1998).
4. V. N. Ngo, H. L. Tang, J. G. Cyster, *ibid.* **188**, 181 (1998).

5. R. Godiska et al., *ibid.* **185**, 1595 (1997); R. J. Rodenburg et al., *J. Leukocyte Biol.* **63**, 606 (1998).
6. M. Chang et al., *J. Biol. Chem.* **272**, 25229 (1997).
7. D. P. Andrew et al., *J. Immunol.* **161**, 5027 (1998).
8. C. Schaniel et al., *J. Exp. Med.* **188**, 451 (1998).
9. BLAST searches of the National Center for Biotechnology Information expressed sequence tag (EST) database for mouse chemokine sequences identified one mouse EST (AA175762) that encoded a 92-amino acid protein with 64% identity to human MDC. This sequence is identical to the recently described mouse ABCD1 sequence (8). An 800-base pair Eco RI fragment containing the coding region was used as a probe for Northern blot analysis, and digoxigenin-based in situ hybridization was performed as described (4). RT-PCR was performed with primers specific for MDC (5'-GTGGCTCTGCTCTCTTGC-3' and 5'-GGACAGTTTATGGAGTAGCTT-3'), ELC (4), or actin. Mature mouse MDC (amino acids 25 to 92) was expressed in *Escherichia coli* as described for ELC (4).
10. T. Imai et al., *J. Biol. Chem.* **273**, 1764 (1998).
11. B. S. Youn et al., *Blood* **89**, 4448 (1997).
12. A. Hoogewerf, D. Black, A. E. Proudfoot, T. N. Wells, C. A. Power, *Biochem. Biophys. Res. Commun.* **218**, 337 (1996).
13. Full-length mouse CCR4 (11, 12) isolated by RT-PCR was subcloned into a modified form of pEF-BOS [S. Mizushima and S. Nagata, *Nucleic Acids Res.* **18**, 5322 (1990)] and transfected into E300-19 pre-B cells (4). The published mouse CCR4 sequences have nine amino acid differences (11, 12). Our sequence matched one or other of the published sequences at each of the nine positions: Ser¹⁴⁵, Glu¹⁸¹, Val²⁴¹, and Phe³¹¹ as in (11) and Ile⁴, Asp²⁰⁵, Cys²²¹, Ala²⁴⁶, and Ala²⁹³ as in (12).
14. H. L. Tang and J. G. Cyster, unpublished observations.
15. T. Imai et al., *J. Biol. Chem.* **271**, 21514 (1996); T. Imai et al., *ibid.* **272**, 15036 (1997).
16. S. Fossum, *Res. Immunol.* **140**, 883 (1989).
17. W. R. Thomas, A. J. Edwards, M. C. Watkins, G. L. Asherson, *Immunology* **39**, 21 (1980); S. E. Macatonia, A. J. Edwards, S. C. Knight, *ibid.* **59**, 509 (1986); S. Hill, A. J. Edwards, I. Kimber, S. C. Knight, *ibid.* **71**, 277 (1990); B. Wang et al., *J. Immunol.* **159**, 6148 (1997).
18. Skin was sensitized as described (17). Mice shown in Fig. 2A were painted on the shaved thorax and abdomen with 0.4 ml of 2% FITC (Sigma) dissolved in a 1:1 (v/v) acetone/dibutyl phthalate (Sigma) mixture, and RNA was prepared from pooled brachial, inguinal, and axillary nodes. For other experiments, a region of mouse skin on the arm or flank was shaved, 25 μ l of 1% FITC in acetone/dibutyl phthalate was applied onto each region, and the draining nodes (brachial and inguinal) were analyzed 1 day later.
19. T. De Smedt et al., *J. Exp. Med.* **184**, 1413 (1996).
20. S. E. Macatonia, S. C. Knight, A. J. Edwards, S. Griffiths, P. Fryer, *ibid.* **166**, 1654 (1987).
21. Mouse ear epidermal cells were isolated and cultured as described (22). In some cases, cells were stained with anti-MHC class II (I-A^b), sorted to >93% MHC class II high LCs, and used for RNA preparation. To purify DCs that were newly migrating into lymph nodes, we painted the skin of mice with FITC (18), and 1 day later, we collected draining lymph nodes and gently mashed them through a 70- μ m mesh cell strainer. DCs in cell suspensions prepared without enzymatic digestion were enriched for FITC⁺ cells, which is consistent with findings that monocyte-derived DCs are more easily isolated from lymphoid tissues than other DC types (7). To prepare RNA, we sorted DCs to >95% B220⁺ FITC⁺ I-A^b-hi cells. For chemotaxis assays, DCs from ~18 FITC-painted mice per experiment were enriched with metrizamide and either immediately put into culture or first sorted to >90% B220⁺ CD11c⁺. Cells were cultured in serum-free medium (Mediatech, Herndon, VA) at 2 \times 10⁶ to 5 \times 10⁶ cells/ml for 1 day. The stromal material that did not enter suspension after mechanical mashing contained SLC-expressing cells and ELC-expressing resident DCs (4, 14). Stromal preparations from 30 to 40 brachial and axillary nodes per experiment were cultured overnight in 2 ml of serum-free medium to provide supernatant for chemotaxis assays.
22. G. Schuler and R. M. Steinman, *J. Exp. Med.* **161**, 526

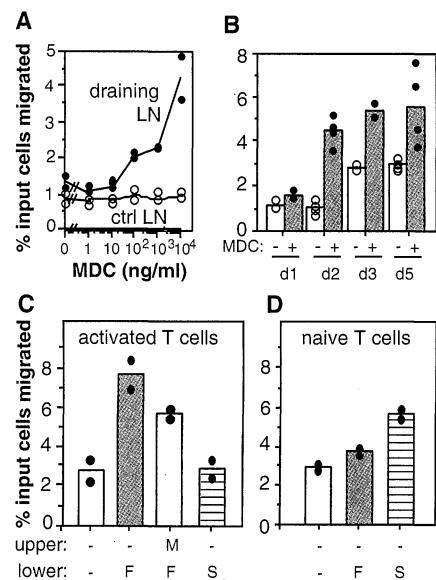


Fig. 4. (A and B) Rapid acquisition of MDC responsiveness in T cells after in vivo activation by antigen. OVA-specific TCR transgenic cells were transferred, and mice were immunized as described (24). Response at day 2 of draining and nondraining (ctrl) lymph node (LN) OVA-specific cells to increasing concentrations of MDC (A). Response of OVA-specific draining lymph node cells to no chemokine (-) or to MDC (10 μ g/ml) (+) at days 1 (d1), 2 (d2), 3 (d3), and 5 (d5) after immunization (B). (C) Chemotaxis of activated T cells to factors secreted by FITC⁺ DC. To the lower transwell chambers, we added supernatant from cultures of no cells (-), sorted FITC⁺ DCs (F) (21), or lymph node stromal cells (S) (27). Responder cells that were added to the upper well in the absence (-) or presence (M) of MDC (1 μ g/ml) were day 2 draining lymph node cells that had been cultured with IL-2 (24). The percentage of input OVA-specific CD4 T cells that migrated from the upper to lower chamber was measured. (D) Chemotaxis of naïve T cells to factors secreted by lymph node stromal cells. Culture supernatants added to lower wells were as in (B). Responder cells were unstimulated lymph node CD4 T cells. Results in (C) and (D) are representative of five experiments.

- (1985); N. Romani *et al.*, *ibid.* **169**, 1169 (1989); C. Heufler *et al.*, *ibid.* **176**, 1221 (1992).
23. R. Bonecchi *et al.*, *ibid.* **187**, 129 (1998).
24. Anti-OVA (DO11.10) T cell receptor (TCR) transgenic lymph node cells (5×10^6 cells) were transferred to BALB/c mice that were immunized 1 day later with 100- μ g OVA in Freund's complete adjuvant (25). Draining (pool of brachial, axillary, and inguinal) and nondraining (mesenteric) lymph node cells were isolated 1 to 5 days later and used in MDC chemotaxis assays. The frequency of OVA-specific T cells that

- migrated was measured with the clonotypic antibody to TCR KJ1-26 (28). Overnight incubation of day 2 draining lymph node cells (at 10^7 cells/ml) in medium containing interleukin-2 (IL-2) (4 ng/ml) increased the sensitivity of activated KJ1-26⁺ cells to MDC (14). Therefore, IL-2-cultured cells were used in experiments to detect chemokine production by purified lymph node DCs and stromal cells.
25. E. R. Kearney, K. A. Pape, D. Y. Loh, M. K. Jenkins, *Immunity* **1**, 327 (1994); K. M. Murphy, A. B. Heimberger, D. Y. Loh, *Science* **250**, 1720 (1990).

26. J. G. Cyster, *J. Exp. Med.* **189**, 447 (1999).
27. G. G. MacPherson, C. D. Jenkins, M. J. Stein, C. Edwards, *J. Immunol.* **154**, 1317 (1995).
28. K. Haskins *et al.*, *J. Exp. Med.* **157**, 1149 (1983).
29. We thank R. Locksley, S. Luther, K. Reif, and A. Weiss for comments on the manuscript; M. Ansel for help with the *in vivo* transfer experiments; and C. McArthur for cell sorting. Supported in part by NIH grant AI-40098, the Pew Foundation (J.G.C.), and the American Lung Association (H.L.T.).

8 January 1999; accepted 23 March 1999

Chaperonin Function: Folding by Forced Unfolding

Mark Shtilerman,¹ George H. Lorimer,^{2*} S. Walter Englander¹

The ability of the GroEL chaperonin to unfold a protein trapped in a misfolded condition was detected and studied by hydrogen exchange. The GroEL-induced unfolding of its substrate protein is only partial, requires the complete chaperonin system, and is accomplished within the 13 seconds required for a single system turnover. The binding of nucleoside triphosphate provides the energy for a single unfolding event; multiple turnovers require adenosine triphosphate hydrolysis. The substrate protein is released on each turnover even if it has not yet refolded to the native state. These results suggest that GroEL helps partly folded but blocked proteins to fold by causing them first to partially unfold. The structure of GroEL seems well suited to generate the nonspecific mechanical stretching force required for forceful protein unfolding.

The GroEL chaperonin (1, 2) captures non-native proteins by means of a ring of hydrophobic residues that line the entrance to the central cavity of its heptameric ring (Fig. 1) (3). When GroEL binds adenosine triphosphate (ATP) and the GroES cochaperonin, a massive structure change doubles the GroEL cavity volume and occludes its hydrophobic binding surface (4, 5). Spectroscopic evidence (6, 7), proteinase protection experiments (6, 8), and electron microscopy (4, 9) leave no doubt that the substrate protein is transiently encapsulated in the central cavity under the GroES lid. However, despite much additional structural and biochemical study (1, 2), the manner in which the GroEL structure change promotes protein folding remains to be demonstrated.

Two models, not mutually exclusive, are under consideration. The Anfinsen cage model (10) is based on the view that protein folding is limited by intermolecular reactions that produce aggregation. The model proposes that the GroEL cavity provides a sequestered microenvironment where folding to the native state can proceed while the substrate protein is protected from aggregation. How-

ever, numerous experiments have shown that the substrate protein is ejected from the cavity with each round of ATP hydrolysis whether it has reached the native state or not (11). The iterative annealing model (12) is based on the view that the rate-limiting step in slow protein folding is the intramolecular reorganization of misfolded and trapped protein segments, dependent on some degree of protein unfolding (13–15). This model proposes that ATP hydrolysis is coupled to a forceful unfolding of the misfolded substrate protein and its release, either into the protected central cavity or to the exterior, so that the misfolding is relieved and forward folding can resume. Incompletely folded proteins undergo further iterations, in the biological equivalent of optimization through annealing (16), until they achieve the native state. However, there is no evidence for a GroES- and ATP-dependent unfolding reaction on the 13-s time scale of the GroEL-adenosine triphosphatase cycle.

We explored GroEL function using unfolded ribulose-1,5-bisphosphate carboxylase-oxygenase (RuBisCO, from *Rhodospirillum rubrum*) labeled by hydrogen-tritium exchange. The role of the individual system components and parameters was studied through their effect on the exchange of the protected RuBisCO hydrogens. Prior studies of GroEL (17–21) used various hydrogen exchange approaches (22). Tritium exchange provides advantages including sensitivity, accuracy, rapidity, and the ability to focus on

one protein within a complex, which allowed us to test the entire active chaperonin system and its individual components on the biologically relevant time scale of seconds.

In nonpermissive conditions RuBisCO folding is blocked. It fails to fold spontaneously (23) and can reach the native state only with the help of the complete GroEL-GroES-ATP system (24). When unfolded RuBisCO is trapped in this way, most of its amide hydrogens exchange rapidly with unlabeled water protons, as expected, but a core of 12 highly protected hydrogens exhibit exchange half-lives of 30 min and longer (detected by tritium label) (Fig. 2). The number of slowly exchanging hydrogens found and their degree of protection ensures that they represent amide groups and not side chains (22). The slowly exchanging hydrogens provide multiple probe sites that are sensitive to structural stability and change and may or may not represent the same sites in different RuBisCO molecules.

The conditions used (pH 8, $22^\circ \pm 2^\circ\text{C}$), chosen to promote the rapid exchange of amide hydrogens that might be transiently unmasked by chaperone action [exchange half-life ~ 10 ms (22)], require that the trapped hydrogens must be highly protected in the non-native protein so that their exchange is slow enough to be measurable. Some other proteins tested provided similar numbers of slow hydrogens but the hydrogens were less protected (maltose-binding protein, malate dehydrogenase, rhodanese) [see also (19)]. It seems likely that the protected RuBisCO hydrogens are sequestered in a partially folded domain. Nevertheless, unfolded RuBisCO retains sufficient non-native structure, perhaps in other domains (25), so that it is efficiently captured by GroEL. The possibility that the slow hydrogens are protected by RuBisCO association or complex formation with GroEL was ruled out by cross-linking experiments that failed to detect RuBisCO association under these conditions and by experiments that compared immediate and delayed GroEL addition.

The time course for exchange of the protected hydrogens is the same for RuBisCO free in solution and when bound to GroEL (Fig. 2A). A similar result was found for unfolded, disulfide-reduced α -lactalbumin (18). To focus on the slowly exchanging hy-

¹The Johnson Research Foundation, Department of Biochemistry and Biophysics, University of Pennsylvania School of Medicine, Philadelphia, PA 19104, USA. ²Department of Chemistry and Biochemistry, University of Maryland, College Park, MD 20742, USA.

*To whom correspondence should be addressed. E-mail: GL48@umail.umd.edu